Structural and magnetic properties of ultrathin fcc Fe films on Cu(001): Full-potential LAPW studies

Xilin Yin and Klaus Hermann
Fritz-Haber-Institut der Max-Planck-Gesellschaft, Faradayweg 4-6, D-14195 Berlin-Dahlem, Germany
(Received 19 July 2000; revised manuscript received 8 December 2000; published 1 March 2001)

Full-potential linearized-augmented-plane-wave calculations using both local-spin-density (LSDA) and generalized gradient Perdew-Burke-Ernzerhof (PBE) functionals are performed to investigate structural and magnetic properties of Cu(001)-Fe film systems with up to three Fe layers. In the calculations full interlayer distance optimizations of the surface systems are carried out allowing both Fe and Cu surface layers to relax. The LSDA calculations yield Fe-Fe and Fe-Cu interlayer spacings which are always smaller compared to Cu bulk, while the PBE results show expanded interlayer distances in agreement with experiment. The supported Fe films are found to be ferromagnetic in the ground state, where the layer-resolved magnetic moments are increased with respect to bulk Fe values. The increase is always largest for the topmost layer and becomes smaller for the sublayers, which is consistent with previous theoretical studies on unrelaxed Cu(001)-Fe systems. In addition, geometry optimizations of Cu(001)-Fe with different spin orientation between the Fe layers show that parallel spin directions of neighboring layers lead to an expanded interlayer distance, whereas antiparallel spin results in contracted interlayer spacing. The geometric effect of interlayer relaxation is found to be significant for the Cu(001)-Fe systems, while magnetic properties of the Fe overlayers are affected less by relaxation.

DOI: 10.1103/PhysRevB.63.115417 PACS number(s): 68.55.Jk, 75.70.Ak, 73.61.At, 71.15.Ap

I. INTRODUCTION

Studies of structural and magnetic properties of iron overlayers on copper substrate have been an attractive subject, and substantial work[1–17] in this field has been carried out in recent years. Experimental studies of Fe film growth on Cu(001) using thermal deposition identify three distinct growth regions by low-energy electron-diffraction (LEED) *I-V* and low-energy ion scattering.[1] In the first region, for coverages ranging from 1 to 4 ML, a complex structure of Fe islands with tetragonal geometry is formed where the lateral interatomic Fe-Fe distances are those of the Cu(001) substrate (1.81 Å), whereas the Fe-Fe interlayer distance is increased compared to the Cu substrate (1.88 Å) as evidenced by LEED investigation.[2] At a coverage of 4 ML Fe forms a complete overlayer film which is ferromagnetic (FM) with perpendicular magnetic anisotropy.[3–5] In the second region, between 5 and 10 ML, the Fe overlayers adopt a fcc structure where, according to LEED *I-V* results,[2] the topmost two interlayer distances are increased ($d_{12}=1.84$ Å and $d_{23}=1.80$ Å) with respect to those of the film interior (1.77 Å). In the third growth region, above 10 ML, the Fe film structure converts gradually to bulk bcc.

Very recently, the pulsed-laser-deposition (PLD) technique was successfully applied to prepare ultrathin Fe films on Cu substrate.[6] This technique provides a layer-by-layer growth mode generating complete Fe overlayer films even for coverages below 2 ML. The PLD films are FM, and the topmost layers are found to be expanded with respect to the average interlayer distance of the Cu substrate.

Extensive theoretical studies have been performed on the Cu(001)-Fe system. Freeman and co-workers[7,8] studied electronic and magnetic properties of thin fcc Fe(001) films with 1 and 2 ML on Cu(001) using the full-potential linearized-augmented-plane-wave (FP-LAPW) method with the local-spin-density approximation (LSDA) functional. For a FM monolayer Fe film on top of Cu(001), their calculations yielded an Fe-Cu interlayer distance which is reduced by about 3% compared to that of fcc Cu. This is also found for the FM double-layer Fe film on Cu(001) where the magnetic moment of the topmost Fe layer is larger than that of the sublayer. Fernando and coworkers [9,10] calculated structural and electronic properties of an epitaxial monolayer Fe film on top of Cu(001) using the film-linearized muffin tin orbital method. They found that the density of states (DOS) of the system remains almost unchanged when the Fe-Cu interlayer spacing is increased by 2% with respect to the Cu-Cu spacing.

Kraft and co-workers[11,12] examined the geometric and magnetic structures of thin fcc Fe films of up to 11 layers on Cu(001) using the full-potential linearized-muffin-tin-orbital method within the LSDA scheme. In their geometry calculations based on total-energy minimization with respect to interlayer distances of the three topmost Fe layers, they found that the surface and first subsurface layers couple ferromagnetically, whereas magnetic coupling is of antiferromagnetic (AFM) nature between deeper lying layers. The calculations yield a 3.9% expansion of the first interlayer spacing, and a 1% contraction of the second. Further, the magnetic structure and anisotropy of fcc Fe overlayers and interlayers at the Cu(001) surface have been studied in fully relativistic spin-polarized Korringa-Kohn-Rostoker calculations within the LSDA framework together with the muffin-tin approximation.[13,14] In these studies no geometric layer relaxation has been taken into account. The authors find that for Fe overlayers, independent of the layer thickness (up to 5 ML), the orientation of the magnetization is always in-plane, while for Fe films capped by Cu layers a perpendicular magnetization is predicted. They also point out that formation of

an AFM fcc Fe ground state is highly sensitive to the atomic volume. Asada and Blügel [3,4] investigated fcc Fe films of up to 6 ML on Cu(001) using the FP-LAPW method (together with the LSDA scheme). In these calculations, they fixed all interlayer distances at $d_{ij}=d_{\text{Cu-Cu}}$, and considered various combinations of spin orientation for the different Fe layers. Their study shows that supported Fe films with up to 3 ML are FM in the ground state whereas thicker films may exhibit both ferromagnetic and AFM coupling.

Despite the abundance of theoretical work on the Cu(001)-Fe system,[3,4,7,8,11,12] previous studies did not include a full optimization of all interlayer spacings of the spin-polarized Fe films and the Cu substrate. Further, in all cases electron exchange and correlation was treated at the LSDA level only. In the present study, we re-examine the electronic and magnetic structure of Fe films with up to 3 ML on Cu(001), where we use the FP-LAPW method together with both LSDA and generalized gradient (GGA) functionals to evaluate total energies as well as the electronic and magnetic structures. The geometric structure of the systems is obtained from total-energy optimizations, where all Fe-Fe, Fe-Cu, and Cu-Cu interlayer spacings are taken into account. Therefore, the present work can help to elucidate the interrelation between geometric layer relaxation and surface magnetic moments in the Fe/Cu system. Further, a comparison of the LSDA results with those using the GGA scheme for electron exchange and correlation can give information about the importance of using different functionals for the present surface systems.

Section II describes computational methods, while Sec. III presents the results and discussion. Here the calculated structural and magnetic properties of Fe thin films on Cu(001) with and without interlayer relaxation are reviewed. Further, the correlation between interlayer spacings and magnetism of the films is discussed in detail. Finally, Sec. IV gives a summary and conclusions.

II. COMPUTATIONAL METHODS

In the present work the Cu(001)-Fe surface system is modeled in repeated slab geometry where the Cu substrate at the (001) surface is described by five layers in fcc geometry with a lateral lattice constant equal to that of the experimental value (at 18 °C), 2.556 Å, (Ref. 18); see below. The approximation of the semi-infinite Cu bulk substrate by a substrate slab of five layers, denoted Cu_5 in the following, is tested in calculations on Cu_n, $n=1,3,\ldots,11$, slab systems, where Cu_5 was found to be a very good compromise between computational effort and numerical accuracy. Epitaxial Fe films of one to three layers are added at both sides of the Cu_5 substrate slab with their starting geometry being equal to that of the fcc Cu substrate. The resulting slabs, denoted $Fe_nCu_5Fe_n$, $n=1$, 2, and 3, in the following, have an inversion symmetry which is made use of in the calculations. The thickness of the vacuum region between adjacent slabs was chosen such that electronic coupling between the slabs could be excluded. Here a value of 8.5 Å proved to be sufficient, as confirmed by test calculations with different vacuum separations. The electronic coupling between the Fe films on both sides of the Cu_5 substrate slab was found to be negligible, as confirmed by comparison of results for $Fe_1Cu_5Fe_1$ with those of $Fe_1Cu_3Fe_1$ and $Fe_1Cu_1Fe_1$ slab systems. In the present work it is assumed that iron forms closed epitaxial 1×1 films on top of the Cu(001) substrate as suggested from the PLD growth experiments.[6] This excludes possible surface alloying and Cu capping of the Fe films, as found in both experimental and theoretical studies on the initial growth of Co on Cu(001).[19,20] However, earlier quantitative LEED analyses[21] gave strong indications that neither surface alloying nor capping will occur in the Cu(001)-Fe system.

The slab studies on the Cu(001)-Fe surface system are complemented by calculations on pure Cu slabs, Cu_n, $n=1,3,\ldots,11$, as models for the Cu(001) surface as well as by pure fcc Fe slabs, Fe_n, $n=1$, and 3, as models of the unsupported Fe films. In all slab calculations the Fe-Fe, Fe-Cu, and Cu-Cu interlayer distances are determined by minimization of total energies and forces on the atoms to obtain equilibrium values. In contrast, the lateral lattice constants of the slabs are kept fixed at the experimental bulk value, which is suggested from LEED studies.[1]

Total energies of the Fe, Cu, and Fe/Cu systems as well as electronic, magnetic, and geometric equilibrium parameters, are determined using the FP-LAPW method[22–24] in repeated slab geometry. Electron exchange and correlation in the spin-polarized systems is accounted for by the LSDA using the Ceperley-Alder[25] functional as well as by the GGA implemented in the Perdew-Burke-Ernzerhof (PBE)[26] functional. The latter includes an accurate description of linear response of the uniform electron gas, correct behavior under uniform scaling, and a smoother potential.[26] In the FP-LAPW method, electron wave functions, densities, and potentials are expanded in spherical harmonics inside muffin-tin (MT) spheres about the atoms while for the interstitial region between the spheres plane-wave expansions are used. The MT sphere radii are chosen to be $R_{\text{MT}}=1.16$ Å for all atoms considered in the present work. For the wave-function representation spherical harmonics with angular momenta up to $l_{\max}=10$ and plane waves up to an energy cutoff of $|\mathbf{K}_{\max}|^2=17$ Ry are employed. For electron densities and potentials we use $l_{\max}=6$ and $|\mathbf{G}_{\max}|^2=144$ Ry. All core electrons are accounted for by a fully relativistic treatment, while valence states are described scalar relativistically.

Restricted geometry optimizations of the slab systems, described above, are based on analytical forces and total energies where 45**k** points in the irreducible part of the Brillouin zone are used in the calculations. The reliability of the geometry optimization was confirmed by separate calculations on ground-state properties of bulk Cu, and of bulk Fe with bcc, fcc, and hcp structures. As an example we mention bulk Cu, where the optimized lattice constant, determined with numerical parameters identical to those of the slab systems, was found to differ from the experimental value, 3.615 Å,[18] by only 0.2%.

III. RESULTS AND DISCUSSION

A. Clean Cu(001) and Fe(001) slabs

As a starting point in the analysis of the Fe/Cu systems, we study the separate components—the clean Cu(001) sub-

TABLE I. Percentage deviation of interlayer distances of fcc Cu(001) slabs with different thicknesses. The values calculated with the PBE functional use a Cu bulk interlayer distance of 1.81 Å as a reference, and are given in a sequence from the topmost Fe layer (left column) to the central Cu layer (right column). Experimental values for the Cu(001) surface are included for comparison.

	$d^{(1)}_{\text{Cu-Cu}}$	$d^{(2)}_{\text{Cu-Cu}}$	$d^{(3)}_{\text{Cu-Cu}}$	$d^{(4)}_{\text{Cu-Cu}}$	$d^{(5)}_{\text{Cu-Cu}}$
Cu_{11}	−2.2	0.6	0.6	0.0	0.0
Cu_9	−2.2	0.6	0.0	0.0	-
Cu_7	−2.2	1.1	0.6	-	-
Cu_5	−2.2	1.1	-	-	-
Cu_3	−1.7	-	-	-	-
expt. (Ref. 27)	−2.8	1.1	0.0	-	-

strate and corresponding unsupported Fe films—by calculations of geometric and electronic properties. Table I lists the percentage deviation of interlayer distances of the fcc Cu(001) slabs with different thickness, where the Cu bulk interlayer distance of 1.81 Å is taken as a reference. The data show that in all cases the topmost layers contract inward (toward the substrate) with respect to their experimental bulk position, where the contraction converges to −2.2% for slabs with five or more layers. In contrast, the first sublayers of each slab are expanded by 0.6% to 1.1%, while deeper lying sublayers are almost unrelaxed. This is in excellent agreement with experimental LEED data for the Cu(001) surface,[27] which yield −2.8% (contraction) for the topmost surface layer, 1.1% (expansion) for the first sublayers and 0% for the second sublayer.

Figure 1 shows the total energies per atom E^{slab}_{tot}/n of the clean Cu(001) slabs with up to 11 layers as a function of slab thickness given by the number n of Cu(001) layers. The energies are taken with respect to the computed value (−3310.064159 Ry) of Cu fcc bulk (obtained with numerical parameters identical to those of the Cu slabs) which is indicated by a dashed line. Obviously, E^{slab}_{tot}/n converges toward the bulk result with increasing slab thickness where for slabs with more than five layers the energy differences are below

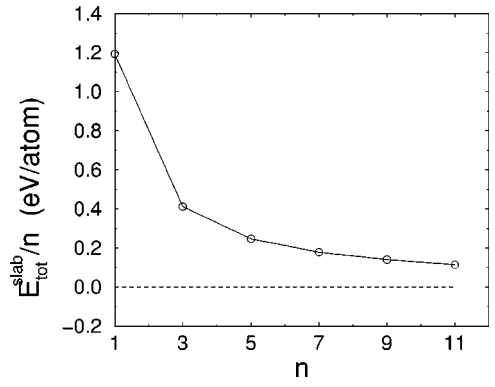

FIG. 1. Total energy per atom E^{slab}_{tot}/n of Cu_n slabs, $n=1-11$, as a function of slab thickness given by the number n of Cu(001) monolayers. The data refer to calculations using the PBE functional. The energy zero, shown by a dashed line, refers to the computed fcc bulk value of Cu.

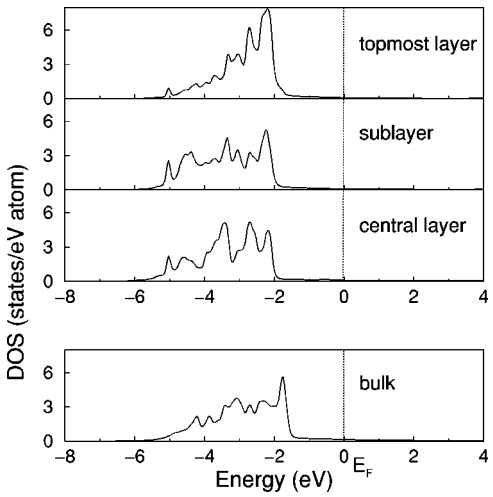

FIG. 2. Layer-projected DOS's for the Cu_5 slab representing the Cu(001) surface. The DOS's, from calculations using the PBE functional, are shown for the three nonequivalent layers (topmost, sublayer, and central). At the bottom, the computed DOS of fcc Cu bulk is given for comparison. All DOS curves have been smoothed by Gaussian broadening with a width of 0.10 eV (full width at half maximum).

0.2 eV. In a first approximation, the elementary cell of a Cu_n slab can be considered as containing two ''surface'' atoms (which experience an incomplete nearest-neighbor shell) and $n-2$ ''bulk'' atoms. Accordingly, the total energy of the cell may be described approximately by

$$E^{slab}_{tot}=2E_{surf}+(n-2)E_{bulk}, \tag{1}$$

where E_{surf} and E_{bulk} are total energies of the surface and bulk atoms, respectively. These energies can be obtained from a fitting procedure based on the calculated E^{slab}_{tot} data. The fit yields error bars for the two energies of only 0.01 eV, which indicates that the above linear relationship for E^{slab}_{tot} is very accurate. This is confirmed by the result that the fitted bulk energy E_{bulk} differs from the value computed for the three-dimensional fcc Cu bulk by only 0.007 eV. The computed energy difference E_{surf}-E_{bulk} amounts to 0.6 eV. The difference between surface and bulk atoms in the slabs also becomes evident in the results of the electronic structure. As an illustration, Fig. 2 shows layer-projected DOS's for the Cu_5 slab (where atomic muffin tin regions of the FP-LAPW calculations were used for the projection). The DOS curves, from calculations with the PBE functional, are shown for the three nonequivalent layers (topmost, sublayer, and central). At the bottom, the computed DOS of fcc Cu bulk is given for comparison. The overall shape of the DOS referring to the topmost layer (consisting of surface atoms) is clearly different from those of the two deeper lying layers (consisting of bulk atoms) whereas the sublayer and central layer DOS's differ by less and are reasonably similar to the Cu bulk DOS. Altogether, the Cu_5 slab results suggest that this system is a good compromise between computational effort and desired accuracy in representing the extended Cu(001) surface.

Table II lists layer-resolved magnetic moments of the Fe monolayer (Fe_1) and the Fe_3 slab with three layers where the

TABLE II. Layer-resolved magnetic moments (in bohr magneton per atom μ_B) of the Fe monolayer (Fe_1) and the Fe_3 slab with optimized inter-layer distances using the PBE and LSDA (in square brackets) functionals. The data are given in a sequence from the topmost Fe layer (left column) to the central Fe layer (right column). The values are compared with previous results on FM fcc and bcc Fe bulk.

	$\mu^{(1)}$	$\mu^{(2)}$	μ
Fe_1	3.06 [3.01]	-	-
Fe_3	2.85 [2.66]	2.62 [1.91]	-
Fe atom	-	-	4.00
Fe bulk (bcc)	-	-	2.35 (2.22) (Ref. 28)
Fe bulk (fcc)	-	-	2.54 (2.47) (Ref. 29)

interlayer distances have been optimized, while the lateral layer geometry is fixed at that of the Cu(001) surface. The calculations using the PBE functional show that the magnetic moment of the topmost layer of the Fe_3 slab is larger than that of the central layer by 9%, but is smaller than that of the Fe monolayer by 7%. All moments of the slabs are larger than respective bulk values, also included in Table II, but are considerably smaller than the free-atom value of $4.0\mu_B$. This is consistent with the general notion that the magnetic moment of an Fe atom is reduced by bond formation with Fe neighbors where the reduction scales with the number of neighbors. Table II also includes magnetic moment results from calculations using the LSDA functional (values in square brackets for the layer systems). The PBE data show qualitatively the same results, with magnetic moments being overall smaller in the LSDA approach. The latter difference is found for all systems of the present study, and cannot be explained by simple physical reasoning. In addition, the moment decrease between the topmost and central layer in the Fe_3 slab is much more pronounced in the LSDA results compared to the PBE results. This is parallel with the much stronger interlayer relaxation found in the LSDA calculations. The optimized interlayer distance computed within the LSDA scheme amounts to 1.55 Å, while the PBE value is 1.86 Å. The origin of this difference is not fully understood, and requires more detailed investigations.

The magnetic moment of bcc bulk determined with the PBE functional ($2.35\mu_B$; see Table II) is larger than the experimental value of $2.22\mu_B$.[28] This can reflect the inaccuracy of the functional but may also be due to numerical influences. As an example, we mention the dependence of the magnetic moment on the actual calculation of the Fermi energy. Using the tetrahedron method results in a numerical moment value ($2.24\mu_B$) very close to experiment, while the value of Table II is calculated using a Fermi-level broadening method which is adopted in the present study in order to achieve better numerical stability for the slab systems.

B. Cu(001)-Fe surface systems

1. Interlayer relaxation

Table III lists the percentage deviation of interlayer distances of the Cu(001)-Fe systems. The Cu bulk interlayer distance of 1.81 Å is taken as a reference, where all values for the $Fe_nCu_kFe_n$ slabs are obtained from spin-polarized calculations using PBE and LSDA functionals (the latter values in parentheses). In all cases, the Fe-Fe and Fe-Cu interlayer distances are found to be expanded, up to 2.4%, with respect to the Cu bulk value when the PBE functional is used in the calculations. In contrast, the LSDA results show considerable contraction, up to -11.6%, in all cases, with contractions being largest for the topmost Fe layer. Further, in the LSDA calculations the contraction continues well inside the Cu substrate slab with Cu-Cu interlayer distances decreased by -2.2 to -5.5% whereas the PBE data show a rapid damping of layer relaxation inside the Cu substrate.

The present LSDA results are in good agreement with other theoretical studies.[3,4,8] A previous LSDA study on the $Fe_1Cu_5Fe_1$ slab system,[8] based on a fully relativistic core and semirelativistic valence electron treatment together with

TABLE III. Percentage deviation of interlayer distances of the Cu(001)-Fe systems. All values for the $Fe_nCu_kFe_n$ slabs use a Cu bulk interlayer distance of 1.81 Å as a reference, and are obtained from spin-polarized calculations with PBE and LSDA functionals (the latter values in parentheses). The table also includes corresponding values for the pure Cu_5 substrate slab and for the $Fe_1Cu_5Fe_1$ slab from spin-averaged (nonmagnetic) calculations as well as LEED results of the Cu(001)-4-ML-Fe film system. The data are given in a sequence from the central Cu layer (left column) to the topmost Fe layer (right column).

	$d^{(2)}_{\text{Cu-Cu}}$	$d^{(1)}_{\text{Cu-Cu}}$	$d_{\text{Fe-Cu}}$	$d^{(1)}_{\text{Fe-Fe}}$	$d^{(2)}_{\text{Fe-Fe}}$
$Fe_3Cu_5Fe_3$	-0.6 (-2.2)	0.0 (-1.7)	1.7 (-0.6)	4.4 (-5.0)	2.2 (-11.6)
$Fe_2Cu_5Fe_2$	-1.1 (-3.3)	0.0 (-3.3)	3.3 (-2.8)	2.2 (-3.3)	-
$Fe_1Cu_5Fe_1$	0.0 (-5.5)	1.1 (-5.5)	0.6 (-6.1)	-	-
$Fe_1Cu_3Fe_1$	-	1.1 (-5.5)	2.2 (-6.1)	-	-
$Fe_1Cu_1Fe_1$	–	–	2.2 (-5.5)	-	-
Cu_5	1.1 (-5.5)	-2.2 (-9.4)	-	-	-
$Fe_1Cu_5Fe_1$ [a]	1.1	1.7	-2.8	-	-
Fe_4/Cu(001) (Ref. 5)	-	-1.7	2.2	5.0	2.8

[a]Results from spin-averaged (nonmagnetic) calculations.

TABLE IV. Layer-resolved magnetic moments (in bohr magnetons μ_B) of the atoms in the Cu(001)-Fe surface systems represented by geometry relaxed and unrelaxed (in parentheses) $Fe_nCu_mFe_n$ slabs using the PBE functional. The atomic moments are given in a sequence from the central Cu layer (left column) to the topmost Fe layer (right column). The three bottom lines list results from previous calculations (Refs. 8 and 13).

	$\mu_{Cu}^{(3)}$	$\mu_{Cu}^{(2)}$	$\mu_{Cu}^{(1)}$	$\mu_{Fe}^{(1)}$	$\mu_{Fe}^{(2)}$	$\mu_{Fe}^{(3)}$
$Fe_3Cu_5Fe_3$	0.00 (0.00)	−0.01 (−0.01)	0.06 (0.07)	2.63 (2.57)	2.64 (2.58)	2.85 (2.86)
$Fe_2Cu_5Fe_2$	0.00 (0.00)	−0.01 (−0.01)	0.06 (0.07)	2.68 (2.61)	2.86 (2.84)	-
$Fe_1Cu_5Fe_1$	0.00 (0.00)	−0.02 (−0.01)	0.05 (0.05)	2.84 (2.83)	-	-
$Fe_1Cu_3Fe_1$	-	−0.02 (−0.02)	0.05 (0.06)	2.87 (2.83)	-	-
$Fe_1Cu_1Fe_1$	-	-	0.10 (0.10)	2.88 (2.84)	-	-
$Fe_3Cu_5Fe_3$	-	-	-	− (2.56) (Ref. 13)	− (2.49) (Ref. 13)	− (2.82) (Ref. 13)
$Fe_2Cu_5Fe_2$ (Ref. 8)	-	-	-	2.60 (2.59 (Ref. 13))	2.85 (2.79 (Ref. 13))	-
$Fe_1Cu_5Fe_1$ (Ref. 8)	-	-	-	2.85 (2.78 (Ref. 13))	-	−

the muffin-tin approximation, yielded a −3% contraction of the Fe-Cu interlayer distance compared to the Cu bulk value. Our calculations (which do not resort to a muffin tin approach) give −6% contraction; see Table III. The difference is clearly due to the different valence electron description due to the muffin tin approach in Ref. 8.

The importance of magnetism (introduced by spin polarization in the calculations) for the film geometry is evident from a comparison of the PBE results of the $Fe_1Cu_5Fe_1$ slab system in its magnetic (spin-polarized) ground state with those where magnetism is artificially quenched by spin averaging. The total energy of the elementary cell of the nonmagnetic state is 1.68 eV above that of the magnetic ground state. Further, the distance of the topmost Fe layer from its nearest Cu sublayer is larger by 0.06 Å in the magnetic state compared to the nonmagnetic one (see Table III), while the distances of the lower-lying (nonmagnetic) Cu sublayers differ by less than 0.01 Å.

LEED experiments on Fe films on Cu(001)[2,5,6,10] show that all Fe-Fe interlayer distances are expanded with respect to the Cu bulk distance (see the bottom line of Table III), while the internal Cu substrate layers remain almost unrelaxed. These findings are in clear disagreement with present and previous LSDA results. In contrast, our PBE calculations on the $Fe_3Cu_5Fe_3$ slab system confirm the experimentally found Fe interlayer expansions rather nicely, even with good quantitative agreement, as is obvious from Table III. This suggests that the use of gradient corrected exchange-correlation functionals, such as the PBE functional is essential in the theoretical treatment of the Cu(001)-Fe system, and can overcome total energy related deficiencies of the LSDA functional.[3,4]

2. Magnetic properties

Table IV lists layer-resolved magnetic moments in the Cu(001)-Fe surface systems represented by geometry optimized and unrelaxed (in parentheses) periodic $Fe_nCu_mFe_n$ slabs using the PBE functional. The PBE results of the $Fe_3Cu_5Fe_3$ and $Fe_2Cu_5Fe_2$ slabs (Table IV), reveal Fe films with FM coupling between the layers in the energetically lowest state. The calculated magnetic moments of the atoms of the topmost Fe layer amount to $2.85\mu_B$ which is very close to the experimental value of $2.8\mu_B$ for Cu(001)-Fe film systems with up to four Fe layers.[1] The magnetic moments of the topmost Fe atoms are always larger than those of the Fe sublayers where the absolute values of all Fe layers are increased with respect to those of the FM bcc Fe bulk, $2.35\mu_B$. The latter is also found for the magnetic moments in the Fe monolayers on Cu(001), slabs $Fe_1Cu_mFe_1$ in Table IV, which are almost identical to the topmost layer moments of the thicker Fe films. Further, the computed PBE moments of the topmost two Fe layers of the $Fe_3Cu_5Fe_3$ slab are very close to corresponding data of the isolated three-layer Fe film; see the Fe_3 results in Table II. This suggests that the enhancement of the magnetic moments found in the Fe films on Cu(001) as compared to bulk Fe is mainly due to electronic coupling within the films while the interaction with the Cu substrate seems to be of minor importance for the magnetic Fe film properties. The largest effect is found for the supported Fe monolayers, where the presence of the Cu substrate reduces the magnetic moments of the atoms in the Fe layer from $3.06\mu_B$ (unsupported film; see Table II) to $2.84\mu_B$. This reduction is mainly due to electronic coupling between the Fe monolayer and the first underlying Cu substrate layer since the thickness of the Cu substrate slab does not seem to influence the magnetic moment of the supported Fe monolayer. This is evident from Table IV, where the moments of the Fe layer for the $Fe_1Cu_mFe_1$, $m=1$, 3, and 5, slabs vary only between $2.84\mu_B$ and $2.88\mu_B$. The magnetic Fe layers induce small magnetic moments in the Cu substrate layers as a result of weak electronic hybridization. This can be seen from Table IV where moments of 0.05 to $0.10\mu_B$ are found for the topmost Cu layer with very rapidly decreasing moments for the underlying sublayers. This is to be expected due to the incomplete *d*-band filling of the Cu substrate.

A comparison of the layer-resolved magnetic moments obtained in calculations using the PBE functional (Table IV), with those based on the LSDA scheme, shows qualitative similarities but detailed quantitative differences. In all cases, the LSDA values of the magnetic moments are smaller than their PBE counterparts. Further, the decay of the layer moments toward the substrate is found to be more rapid in the

LSDA approach compared to the PBE approach. These discrepancies, due to the use of different approximations in the electron exchange/correlation treatment, can be described by two interrelated contributions. First, the electronic structure calculation for a given film geometry must result in magnetic moments which depend on the exchange/correlation functional. Second, the equilibrium geometries of the film systems differ somewhat between the PBE and LSDA optimizations; see Sec. III B 1 and Table III. An analysis of the two contributions becomes possible by calculations using identical geometries and different functionals or identical functionals and different geometries, as will be discussed below.

The present LSDA results of layer−resolved magnetic moments of the $Fe_2Cu_5Fe_2$ and $Fe_1Cu_5Fe_1$ slabs are in good agreement with other theoretical studies.[7,8] These studies yield moments which are larger than those of the present calculations by only $0.10\mu_B$ to $0.13\mu_B$ where the differences may be explained by the different valence electron treatment in the two studies as discussed in Sec. III B 1.

Table IV lists computed layer−resolved magnetic moments of unrelaxed $Fe_nCu_mFe_n$ slabs, where the interlayer distances between Cu layers are fixed at the Cu bulk value and those between Fe layers as well as the Fe−Cu interlayer distance are frozen at the bulk value of fcc Fe. The data are obtained from calculations using the PBE functional. A detailed comparison of the magnetic moment results between the optimized and unrelaxed geometries gives a clear picture of the influence of interlayer displacements on the layer−resolved magnetic moments. The PBE derived moments differ between the optimized and unrelaxed geometries for all systems of this study by only $0.01\mu_B$ to $0.07\mu_B$. This suggests that for interlayer distance variations which are typical for surface relaxation, layer−resolved magnetic moments experience only small changes. Clearly, these changes become larger for larger interlayer distance variations. This was studied in test calculations on the $Fe_2Cu_5Fe_2$ slab system where, starting from the equilibrium interlayer geometry, the topmost Fe layer is varied in its position with the other layers kept fixed. Figure 3 shows the layer−resolved magnetic moments of the two Fe layers as a function of the Fe−Fe interlayer distance. The moment of the topmost Fe layer converges toward the value of the unsupported Fe monolayer, $3.06\mu_B$, for distances beyond 1 Å above the equilibrium distance. At the same time, the magnetic moment of the second Fe layer assumes the value of the Fe layer in the $Fe_1Cu_5Fe_1$ slab, $2.84\mu_B$. Both limits are reasonable, and reflect the situation of an isolated Fe monolayer on top of an $Fe_1Cu_5Fe_1$ slab. At Fe−Fe separations smaller than 0.2 Å below the equilibrium distance, the magnetic moments of both Fe layers are quenched substantially with large moment variations. However, there is a distance region of ±0.1 Å about the equilibrium distance in which the magnetic moments vary by $0.05\mu_B$ at most. This distance range corresponds to typical values for surface relaxation. In the present calculations, contributions to the magnetic moment due to spin−orbit coupling are not included. Previous fully relativistic studies on the $Fe_1Cu_5Fe_1$ system yielded spin and orbital moment contributions (accounting for both spin−orbit coupling and spin polarization, where the latter is included in the present calculations) of the top Fe layer of only $0.126\mu_B$.[30] Thus we estimate that the present magnetic moment values have to be corrected by less than $0.1\mu_B$ in order to account for spin−orbit coupling effects.

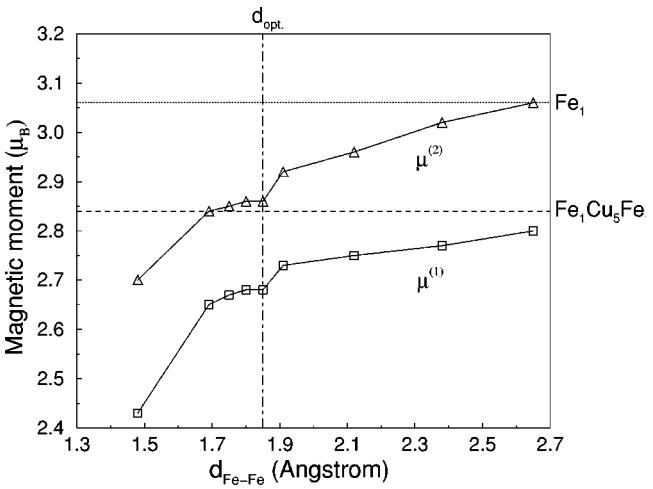

FIG. 3. Layer−resolved magnetic moments of the two Fe layers of the $Fe_2Cu_5Fe_2$ slab as a function of the Fe−Fe interlayer distance when the topmost Fe layer is removed from the slab. Here $\mu^{(2)}$ is the moment of the topmost Fe layer, and $\mu^{(1)}$ that of the second Fe layer. The dashed horizontal line denotes the magnetic moment of the Fe layer in the $Fe_1Cu_5Fe_1$ slab, while the dotted line gives the magnetic moment of an unsupported Fe monolayer. The data refer to calculations using the PBE functional. The distance $d_{\text{opt.}}$ defines the optimized geometry of the $Fe_2Cu_5Fe_2$ slab.

3. Fe films of different magnetic ordering on Cu(001), geometric consequences

It was mentioned above that the energetically lowest states of the two− and three−layer Fe films on Cu(001), represented by $Fe_2Cu_5Fe_2$ and $Fe_3Cu_5Fe_3$ slabs, yield FM coupling (parallel spins) between the Fe layers which is consistent with experiment.[5,6,15] It is also interesting to examine excited states of these films where both FM and AFM coupling between the layers can appear and is combined with different equilibrium interlayer distances.

Table V, part (a), collects optimized interlayer distances $d^{(i)}_{A-B}$ and total energies of the $Fe_2Cu_5Fe_2$ and $Fe_3Cu_5Fe_3$ slab systems for different states of magnetic ordering. In addition, Table V, part (b), lists layer−resolved magnetic moments from the spin−polarized calculations using the PBE functional. Here the different states are described by the relative spin orientation of their Fe layers (u, up; d, down). An inspection of the total energies of the two−layer Fe film systems confirms that the FM order (uu) refers to the energetically lowest state while AFM ordering (ud) requires an excitation energy of 0.5 eV with respect to the ground state. This is consistent with previous work[3–8,15] based on the LSDA functional. As an example, we mention previous studies[8] which yielded an excitation energy of 0.2 eV. The three−layer Fe film systems allow four different spin orientations of their layers: uuu, uud, udd, and udu, where the complete FM order (uuu) represents the energetically lowest

TABLE V. Percentage deviation of interlayer distances with respect to the Cu bulk interlayer distance of 1.81 Å (a) and layer−resolved magnetic moments (in bohr magnetons μ_B) (b) of the $Fe_2Cu_5Fe_2$ and $Fe_3Cu_5Fe_3$ slab systems for different states of magnetic ordering. The states are characterized by the relative spin orientation of their Fe layers (u, up; d, down). All values are obtained from spin−polarized calculations using the PBE functional. The sequence of the values is from the central Cu layer (left column) to the topmost Fe layer (right column). The last column of (a) lists total energies E_{tot} (in eV per unit cell, with respect to the ground state) of the different states and compares with previous work (Refs. 3 and 8). Spin−up moments are given by positive values, while spin−down moments refer to negative values. (b) also contains numerical results from previous LSDA calculations on $Fe_2Cu_5Fe_2$ slabs (Ref. 8).

(a) Optimized interlayer distances

	$d^{(2)}_{Cu-Cu}$	$d^{(1)}_{Cu-Cu}$	d_{Cu-Fe}	$d^{(1)}_{Fe-Fe}$	$d^{(2)}_{Fe-Fe}$	E_{tot} (eV)
$Fe_2Cu_5Fe_2$						
uu	−1.1	0.0	3.3	2.2	-	0.00 / 0.00 (Ref. 8)
ud	0.0	0.0	2.2	−5.0	-	0.52 / 0.21 (Ref. 8)
$Fe_3Cu_5Fe_3$						
uuu	−0.6	0.0	1.7	4.4	2.2	0.00 / 0.00 (Ref. 3)
uud	−0.6	0.0	1.7	−2.8	1.1	0.07 / 0.11 (Ref. 3)
udd	−1.1	0.0	1.1	3.3	−4.4	0.33 / 0.64 (Ref. 3)
udu	0.0	1.1	2.2	−5.0	−6.6	0.38 / 0.88 (Ref. 3)

(b) Layer−resolved magnetic moments

	$\mu^{(3)}_{Cu}$	$\mu^{(2)}_{Cu}$	$\mu^{(1)}_{Cu}$	$\mu^{(1)}_{Fe}$	$\mu^{(2)}_{Fe}$	$\mu^{(3)}_{Fe}$
$Fe_2Cu_5Fe_2$						
uu	0.00	−0.01	0.06	2.68 (2.60 (Ref. 8))	2.86 (2.85 (Ref. 8))	-
ud	0.00	0.01	−0.06	−2.20 (−2.22 (Ref. 8))	2.40 (2.38 (Ref. 8))	-
$Fe_3Cu_5Fe_3$						
uuu	0.00	−0.01	0.06	2.63	2.64	2.85
uud	0.00	0.01	−0.06	−2.21	2.35	2.86
udd	0.00	0.00	−0.07	−2.64	−2.27	2.42
udu	0.00	−0.01	0.06	2.24	−0.99	2.49

state. The lowest excited state, at only 0.07 eV above the ground state, is described by a spin flip in the third Fe layer of the film which is closest to the Cu substrate. This is accompanied by a reduction of the absolute magnetic moments of the second and third Fe layers as seen from Table V, part (b). The second excited state (udd), at 0.3 eV above the ground state, is characterized by AFM coupling between the first and second Fe layers, and FM coupling between the second and third layers. Finally, the third excited state (udu), at 0.4 eV, reveals AFM coupling between all adjacent Fe layers. The energetic order of the four different magnetic states is identical to that obtained in a previous study[3] where, however, excitation energies were found to be larger than the present values [see Table V, part (a)], which is explained by the use of both the LSDA functional and unrelaxed layer geometries in the previous study.

A comparison of the equilibrium Fe−Fe interlayer distances for the different magnetic order states, given in Table V, part (a), reveals an interesting correlation between spatial geometry and magnetic ordering. As an example, the $Fe_2Cu_5Fe_2$ slab system yields in its ground state (uu), where the two Fe layers couple ferromagnetically, optimized Fe−Fe interlayer distances which are expanded with respect to the Cu bulk interlayer distance. In contrast, in the excited state (ud) with AFM Fe−Fe layer coupling the interlayer distance is reduced. This qualitative finding—that FM interlayer coupling results in interlayer expansion while AFM coupling yields interlayer compression—can be found in all Cu(001)−Fe layer systems considered in this study. It can also be observed in the results of previous LSDA studies on thicker Fe films,[3,4,11,12] and seems to be of general validity. The present correlation between spatial geometry and magnetic ordering may be connected with the magnetic pressure effect, which was discussed in connection with the thermal expansion behavior of invar materials.[31,32] However, more detailed studies are required to explain the present correlation in detail.

IV. CONCLUSIONS

The present FP−LAPW calculations give valuable insight into magnetic and structural properties of the present Cu(001)−Fe film systems with up to three Fe layers. In this study full interlayer distance optimizations of the surface systems are carried out, allowing both Fe and Cu surface layers to relax freely (to our knowledge this was ignored or included only in an approximate fashion in previous studies[3,4,7,8,11–14]). This can give an unbiased estimate of the interplay between geometric structure and magnetic properties in the Cu(001)−Fe film systems. Further, in the present study the electronic structure is determined by FP−LAPW slab calculations, using both the LSDA functional for ex-

change and correlation (applied exclusively in all previous studies) and the more recent gradient corrected PBE functional. The comparison of the LSDA and PBE results can give insight into the importance of the use of different functionals for the geometric structure and magnetic properties in Cu(001)−Fe film systems.

The optimization of interlayer distances in the Cu(001)−Fe film systems using the PBE functional results in layer−spacing expansions which are even quantitatively very similar to measured relaxations.[5] In contrast, the LSDA data lead to contraction of all Fe layers. This suggests that the use of gradient−corrected exchange−correlation functionals, such as PBE functionals, is essential in the theoretical treatment of the Cu(001)−Fe system, and can overcome total energy related deficiencies of the LSDA functional.[3,4]

A comparison of the magnetic moment results obtained from calculations using the PBE functional with those using the LSDA functional yields qualitative agreement where, in all cases, the LSDA values for the topmost Fe layers are smaller than their PBE counterparts by $0.10\mu_B$ to $0.15\mu_B$. This is important for a comparison with experiment,[1] where the PBE results agree better when spin−orbit coupling contributions are ignored. Both functionals always yield FM ground states where the layer−resolved magnetic moments per atom are increased with respect to those of bulk Fe. The increase is largest for the topmost layer, and becomes smaller for the sublayers, which is consistent with previous LSDA studies on unrelaxed Cu(001)−Fe systems.[7,8] The enhancement of the magnetic moments is considered to be due mainly to electronic coupling within the films, while the interaction with the Cu substrate seems to be of minor importance.

Calculations on excited magnetic states of the Cu(001)−Fe film systems where both ferromagnetic (FM) and antiferromagnetic (AFM) coupling between the layers is allowed, show an interesting correlation between spatial geometry and magnetic ordering. FM coupling between adjacent layers results in interlayer expansion, while AFM coupling yields interlayer compression. This correlation was observed in all Cu(001)−Fe layer systems of the present study, and seems to be of general validity. It may be connected with the magnetic pressure effect, discussed for invar materials.[31,32] However, more detailed studies are required to explain this interesting finding. Calculations along these lines are presently under way.

ACKNOWLEDGMENTS

We would like to thank M. Scheffler and X.−G. Wang for valuable discussions and advice. This work was supported by the DFG through SFB 290, ''Metallic Thin Films: Structure, Magnetism, and Electronic Properties.''

[1] D. Schmitz, C. Charton, A. Scholl, C. Carbone, and W. Eberhardt, Phys. Rev. B **59**, 4327 (1999).
[2] A. Clarke, P. J. Rous, M. Arnott, G. Jennings, and R. F. Willis, Surf. Sci. **192**, L843 (1987).
[3] T. Asada and S. Blügel, Phys. Rev. Lett. **79**, 507 (1997).
[4] T. Asada and S. Blügel, J. Magn. Magn. Mater. **177−181**, 1233 (1998).
[5] S. Müller, P. Bayer, C. Reischl, and K. Heinz, Phys. Rev. Lett. **74**, 765 (1995).
[6] H. Jenniches, J. Shen, Ch. V. Mohan, S. Sundar Manoharan, J. Barthel, P. Ohresser, M. Klaua, and J. Kirschner, Phys. Rev. B **59**, 1196 (1999).
[7] M. F. Onellion, C. L. Fu, M. A. Thompson, J. L. Erskine, and A. J. Freeman, Phys. Rev. B **33**, 7322 (1986).
[8] C. L. Fu and A. J. Freeman, Phys. Rev. B **35**, 925 (1987).
[9] G. W. Fernando, Y. C. Lee, P. A. Motano, B. R. Cooper, E. R. Moog, H. M. Naik, and S. D. Bader, J. Vac. Sci. Technol. A **5**, 882 (1987).
[10] G. W. Fernando and B. R. Cooper, Phys. Rev. B **38**, 3016 (1988).
[11] T. Kraft, P. M. Marcus, and M. Scheffler, Phys. Rev. B **49**, 11 511 (1994).
[12] T. Kraft, Ph.D. thesis, TU Berlin, 1994, ISBN 3−929937−69−7.
[13] L. Szunyogh, B. Ujfalussy, and P. Weinberger, Phys. Rev. B **55**, 14 392 (1997).
[14] B. Ujfalussy, L. Szunyogh, and P. Weinberger, Phys. Rev. B **54**, 9883 (1996).
[15] Th. Detzel, M. Vonbank, M. Donath, N. Memmel, and V. Dose, J. Magn. Magn. Mater. **152**, 287 (1996).
[16] M. Wuttig and J. Thomassen, Surf. Sci. **282**, 237 (1993).
[17] D. P. Pappas, K.−P. Kämper, B. P. Miller, H. Hopster, D. E. Fowler, A. C. Luntz, C. R. Brundle, and Z.−X. Shen, J. Appl. Phys. **69**, 5209 (1991).
[18] R. W. G. Wyckoff, *Crystal Structures*, 2nd ed. (Wiley, New York, 1982).
[19] F. Nouvertné, U. May, M. Bamming, A. Rampe, U. Korte, and G. Güntherodt, Phys. Rev. B **60**, 14 382 (1999).
[20] R. Pentcheva and M. Scheffler, Phys. Rev. B **61**, 2211 (2000).
[21] K. Heinz, S. Müller, and P. Bayer, Surf. Sci. **337**, 215 (1995).
[22] P. Blaha, K.−H. Schwarz, P. Sorantin, and S. B. Trickey, Comput. Phys. Commun. **59**, 399 (1990).
[23] B. Kohler, S. Wilke, M. Scheffler, R. Kouba, and C. Ambrosch−Draxl, Comput. Phys. Commun. **94**, 31 (1996).
[24] M. Petersen, F. Wagner, L. Hufnagel, M. Scheffler, P. Blaha, and K.−H. Schwarz, Comput. Phys. Commun. **126**, 294 (2000).
[25] D. M. Ceperley and B. J. Alder, Phys. Rev. Lett. **45**, 566 (1980).
[26] J. P. Perdew, K. Burke, and M. Ernzerhof, Phys. Rev. Lett. **77**, 3865 (1996).
[27] Q. T. Jiang, P. Fenter, and T. Gustafsson, Phys. Rev. B **44**, 5773 (1991).
[28] C. Kittel, *Introduction to Solid State Physics*, 6th ed. (Wiley, New York, 1986).
[29] C. S. Wang, B. M. Klein, and H. Krakauer, Phys. Rev. Lett. **54**, 1852 (1985).
[30] O. Hjortstam, J. Trygg, J. M. Wills, B. Johansson, and O. Eriksson, Phys. Rev. B **53**, 9204 (1996).
[31] E. F. Wassermann, J. Magn. Magn. Mater. **100**, 346 (1991).
[32] M. Podgorny and J. Goniakowski, Nuovo Cimento D **13**, 311 (1991).